SMC-TR-03-22

AEROSPACE REPORT NO.
TR-2003(8555)-3

# Battery Voltage Fluctuations during Penumbral Passage

20 June 2003

Prepared by

A. H. ZIMMERMAN
Electronics and Photonics Laboratory
Laboratory Operations

Prepared for

SPACE AND MISSILE SYSTEMS CENTER
AIR FORCE SPACE COMMAND
2430 E. El Segundo Boulevard
Los Angeles Air Force Base, CA 90245

Engineering and Technology Group

THE AEROSPACE CORPORATION
El Segundo, California

This report was submitted by The Aerospace Corporation, El Segundo, CA 90245-4691, under Contract No. F04701-00-C-0009 with the Space and Missile Systems Center, 2430 E. El Segundo Blvd., Los Angeles Air Force Base, CA 90245. It was reviewed and approved for The Aerospace Corporation by B. Jaduszliwer, Principal Director, Electronics and Photonics Laboratory. Michael Zambrana was the project officer for the Mission-Oriented Investigation and Experimentation (MOIE) program.

This report has been reviewed by the Public Affairs Office (PAS) and is releasable to the National Technical Information Service (NTIS). At NTIS, it will be available to the general public, including foreign nationals.

This technical report has been reviewed and is approved for publication. Publication of this report does not constitute Air Force approval of the report's findings or conclusions. It is published only for the exchange and stimulation of ideas.

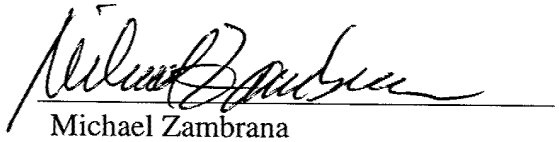

Michael Zambrana
SMC/AXE

# REPORT DOCUMENTATION PAGE

Form Approved
OMB No. 0704-0188



| 1. REPORT DATE (*DD-MM-YYYY*) | 2. REPORT TYPE | 3. DATES COVERED *(From - To)* |
|---|---|---|
| 20-06-2003 | | |

**4. TITLE AND SUBTITLE**

Battery Voltage Fluctuations during Penumbral Passage

**5a. CONTRACT NUMBER**
F04701-00-C-0009

**5b. GRANT NUMBER**

**5c. PROGRAM ELEMENT NUMBER**

**6. AUTHOR(S)**

A. H. Zimmerman

**5d. PROJECT NUMBER**

**5e. TASK NUMBER**

**5f. WORK UNIT NUMBER**

**7. PERFORMING ORGANIZATION NAME(S) AND ADDRESS(ES)**

The Aerospace Corporation
Laboratory Operations
El Segundo, CA 90245-4691

**8. PERFORMING ORGANIZATION REPORT NUMBER**

TR-2003(8555)-3

**9. SPONSORING / MONITORING AGENCY NAME(S) AND ADDRESS(ES)**

Space and Missile Systems Center
Air Force Space Command
2450 E. El Segundo Blvd.
Los Angeles Air Force Base, CA 90245

**10. SPONSOR/MONITOR'S ACRONYM(S)**
SMC

**11. SPONSOR/MONITOR'S REPORT NUMBER(S)**
SMC-TR-03-22

**12. DISTRIBUTION/AVAILABILITY STATEMENT**

Approved for public release; distribution unlimited.

**13. SUPPLEMENTARY NOTES**

**14. ABSTRACT**

The effect of power system load fluctuations on nickel-hydrogen battery cell voltage has been examined during simulated transit from discharge to charge as a satellite traverses a penumbral region of space. The types of cell and battery resistances that can affect the voltage ripple are identified and measured for an aged 60-Ah nickel-hydrogen cell, and are found to range from 0.95 to 1.25 V for a 22-cell battery for 30-A load fluctuations. The highest voltage ripple occurs at the lowest battery state of charge and at the lowest battery temperature. These measurements provide voltage regulation guidelines for satellite power systems.

**15. SUBJECT TERMS**

Battery, Voltage ripple, Penumbra, Resistance

| 16. SECURITY CLASSIFICATION OF: | | | 17. LIMITATION OF ABSTRACT | 18. NUMBER OF PAGES | 19a. NAME OF RESPONSIBLE PERSON |
|---|---|---|---|---|---|
| a. REPORT | b. ABSTRACT | c. THIS PAGE | | 9 | Albert Zimmerman |
| UNCLASSIFIED | UNCLASSIFIED | UNCLASSIFIED | | | 19b. TELEPHONE NUMBER *(include area code)* (310)336-7415 |

## Contents

1. Introduction ..... 1
2. Test Description ..... 3
3. Analysis of Data ..... 7
5. Battery Voltage Ripple Implications ..... 9
4. Conclusions ..... 11

## Figures

1. Recharge behavior of 60-Ah test cell during the three cycles conducted. ..... 4
2. Discharge behavior of 60-Ah test cell during the three cycles conducted. ..... 4
3. Typical pulses at end of charge between +6 A and –15 A at 10°C. ..... 5
4. Typical pulses at end of discharge between –15 A and –15 A at 10° C. ..... 5
5. Voltage transients recorded at 0°C when applying +15 A of charge current after discharging 18 Ah of capacity from a 60-Ah cell. ..... 7
6. Voltage transients recorded at 10°C when applying +15 A of charge current after discharging 18 Ah of capacity from a 60-Ah cell. ..... 8

## Tables

1. Resistances Obtained for a 60-Ah $NiH_2$ Cell at EOL for the Transition from C/4 Discharge to C/4 Charge ..... 8
2. Voltage Ripple Estimates for a 22-Cell 60-Ah $NiH_2$ Battery with No External Cell Wiring Resistance ..... 9

# 1. Introduction

As a satellite passes into or out of eclipse shadowing, the solar array passes through a penumbral region of space where it is only partially illuminated. During this period, the satellite electrical loads ideally shift smoothly from battery power to solar array power. However, a smooth load shift of this kind requires that the satellite loads do not change rapidly with time during the penumbral transit. If the satellite loads shift significantly during the penumbral transit, which lasts on the order of 10 s, the batteries can experience alternating charge and discharge current pulses. In the case where direct energy transfer from the batteries to the bus is used, the alternating charge and discharge pulses can cause the battery to apply a voltage ripple to the satellite power bus. Here we evaluate the magnitude of the battery voltage ripple based on test data obtained from a 60-Ah nickel-hydrogen cell.

## 2. Test Description

The cell used in these tests was an RNH 60-5 nickel-hydrogen cell manufactured by Eagle-Picher Technologies in Joplin, MO. The cell was built with a dual-layer Zircar separator, and was activated with 31% KOH electrolyte. Prior to these tests, this cell was subjected to approximately 15,000 life test cycles at 60% depth of discharge (DOD). The cell was also subjected to extensive high-rate overcharge at several times during the cycling, which led to significant capacity loss and failure to support a 60% DOD LEO cycle. The cell capacity had dropped to about 45–50 Ah after the cycling test. The cell was then stored in a fully discharged state at ambient temperature about two years before the testing reported here. The cell was stored with significant hydrogen precharge that had built up during the cycling test, and thus experienced some additional capacity loss. At the time of these tests, this 60-Ah cell delivered approximately 40 Ah of capacity. It is clearly representative of a nickel-hydrogen cell at end of life. In this report, all depths of discharge are determined based on the actual capacity of the cell, which is about 40 Ah. The C rate for this cell is 60 A.

This cell was maintained at nominal temperatures of either 0°C or 10° C for these tests in a liquid-filled coolant reservoir. A bipolar power supply (KEPCO 20-20M) having a 0.1-ms current rise time was used in these tests. Before any tests were done, a wakeup cycle consisting of a C/10 recharge for 16 h, followed by a C/4 discharge to 1.0 V was performed. Prior to each subsequent test, the cell was recharged for 16 h at a C/10 charge rate.

The cell voltage fluctuations were measured in response to C/4 charge and C/4 discharge pulses that were applied to the cell at the end of discharge at several depths of discharge. Eight charge and discharge pulses, each lasting 0.5 s, were applied to the cell while the cell voltage was monitored with 18 ms time resolution. In addition, the effect of pulse load fluctuations was examined at the end of recharge in response to C/10 charge and C/4 discharge pulses that were applied to the cell at the end of charge when the cell was at 100% state of charge.

The charge voltage behavior of the cell is indicated in Figure 1 for the three cycles performed during the testing reported here, and the discharge voltage behavior is reported in Figure 2. The first of these cycles was a wakeup cycle at 0°C with an 18-Ah discharge. The second cycle was at 10°C, and involved full recharge at C/10 followed by full discharge at a C/4 rate. The third cycle was at 0°C,

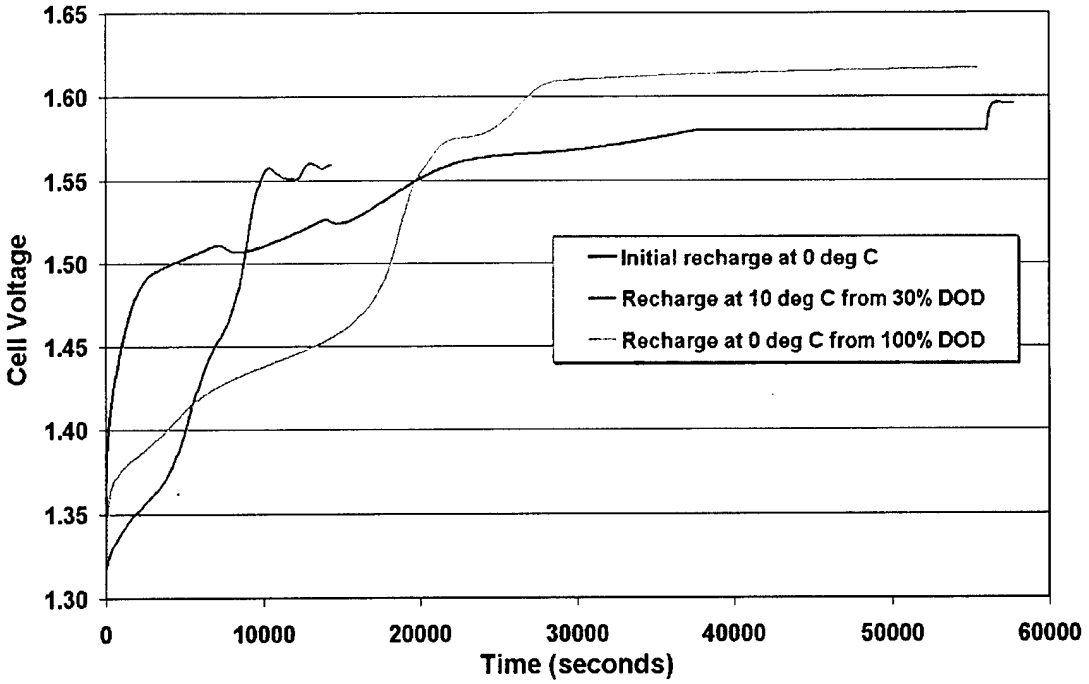


Figure 1. Recharge behavior of 60-Ah test cell during the three cycles conducted.

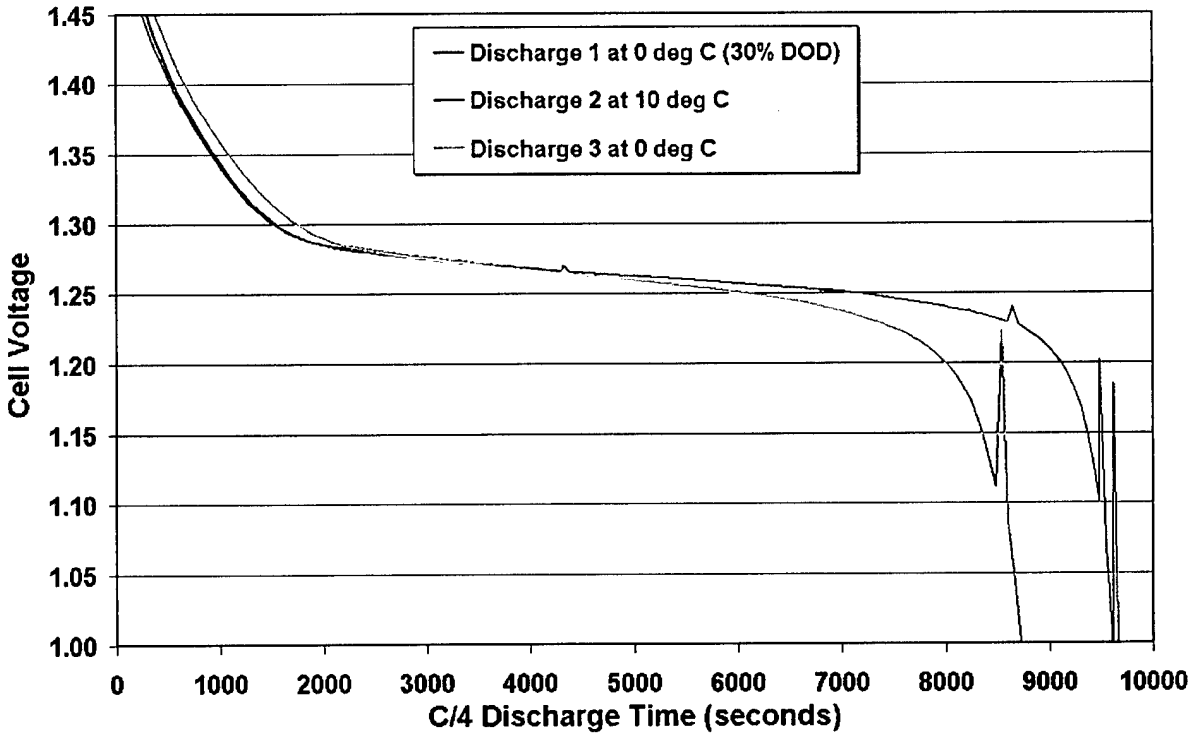


Figure 2. Discharge behavior of 60-Ah test cell during the three cycles conducted.

and involved full recharge at C/10 followed by full discharge at a C/4 rate. Figures 3 and 4 show typical voltage responses to the cell load fluctuations at the end of recharge and after a C/4 discharge for 1.2 h (~ 55% SOC, 18 Ah discharged), respectively.

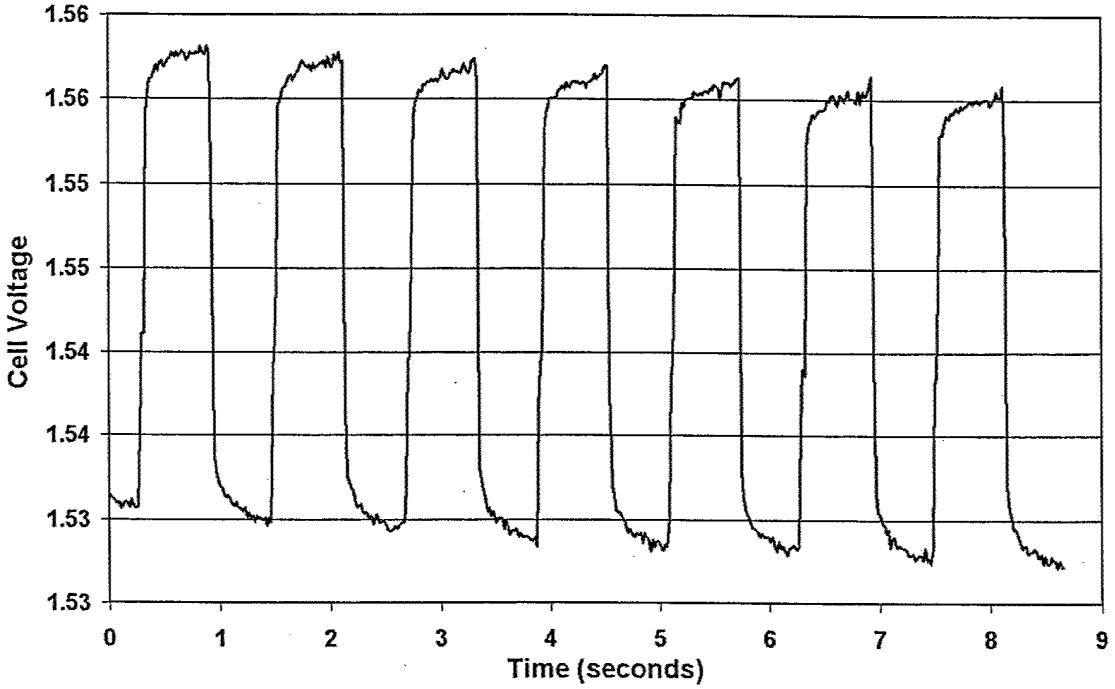


Figure 3. Typical pulses at end of charge between +6 A and –15 A at 10°C.

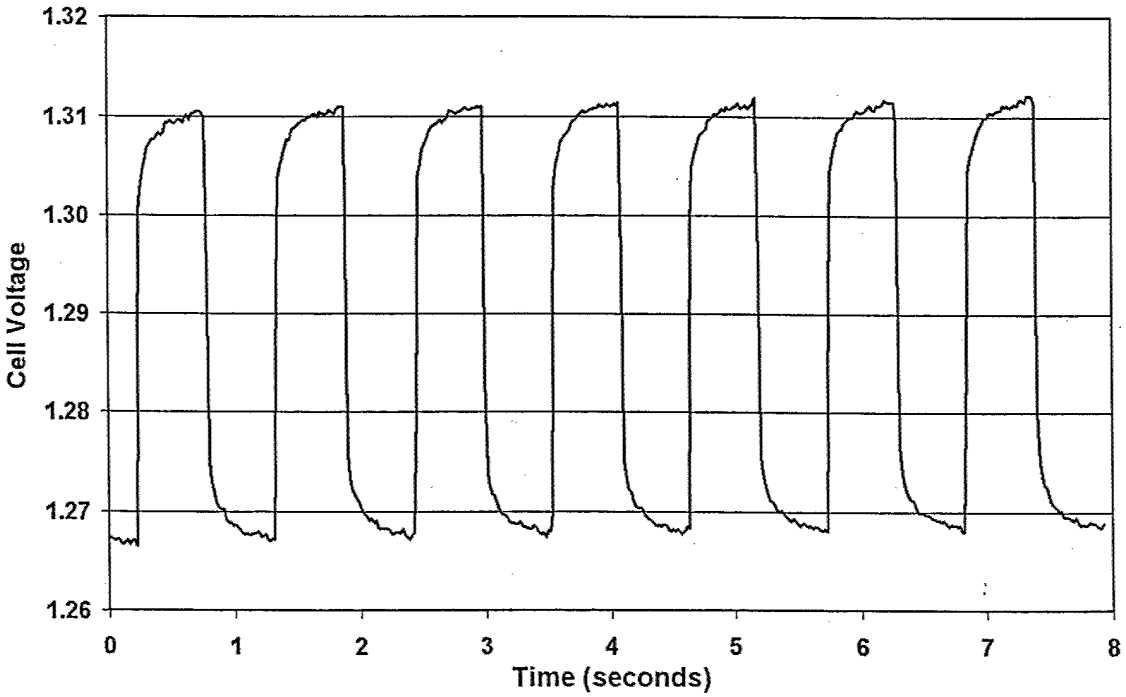


Figure 4. Typical pulses at end of discharge between +15 A and –15 A at 10°C.

## 3. Analysis of Data

Pulse data such as that shown in Figures 3 and 4 were analyzed to extract two types of resistance. The first, referred to as $R_{cell}$, corresponds to the high-frequency (~500 Hz) impedance of the cell, and corresponds essentially to the resistance of the leads and the electrolyte. In the pulse measurements obtained here, this resistance causes the instantaneous voltage drop in response to the current change. $R_{cell}$ is typically about 1 mΩ for a nickel-hydrogen cell, and may vary depending on the design of a cell or battery conductors. The second type of resistance, $R_{pol}$, corresponds to the polarization of the electrodes over the 0.5-s interval that a current transient is applied. $R_{pol}$ will increase as the time is extended from when the current transient was applied and will decrease as the currents are increased, but will be similar for all cells using nickel electrodes of the same generic design.

Figure 5 shows typical voltage transients recorded at 0°C and different states of charge, and Figure 6 shows similarly recorded data at 10°C. In Figures 5 and 6, the voltage transient is plotted vs. the square root of time, since the diffusive polarization processes lend themselves to linear extrapolation in such a plot. $R_{cell}$ is obtained from these transients by fitting the voltage measurements just prior to initiation of the transient to a linear function, and also by fitting the voltage measurements just after the application of the transient to a linear function. At the instant when the transient was applied, the difference between these two linear functions, when divided by the change in current, provides $R_{cell}$. The difference between the pre-transient voltage and the voltage after 0.5 s, when divided by the change in current, provides $R_{cell} + R_{pol}$. Table 1 indicates the resistances that were obtained.

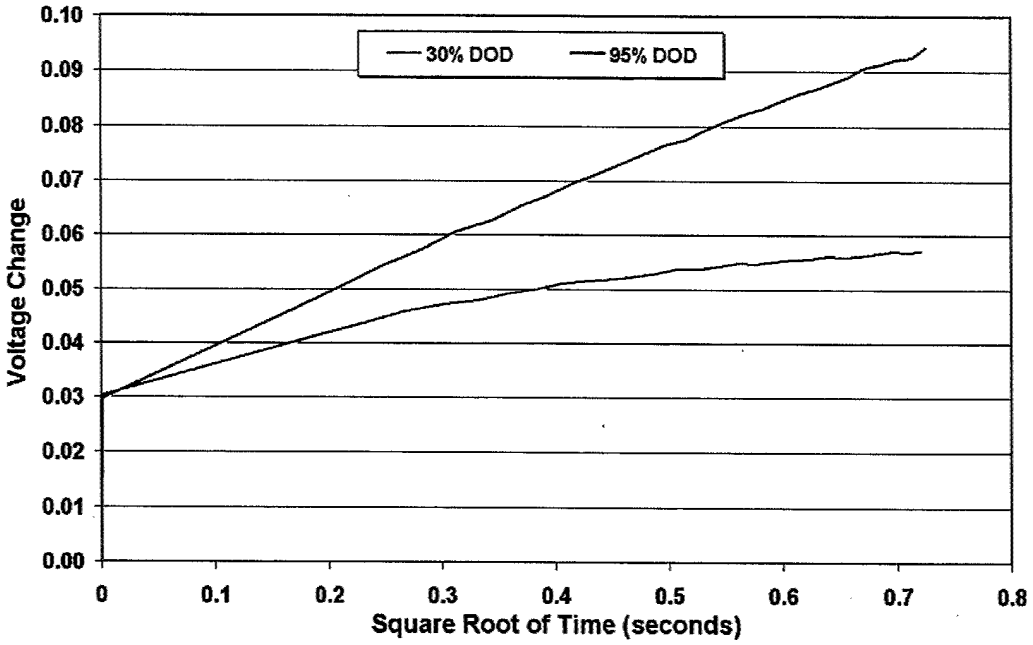


Figure 5. Voltage transients recorded at 0°C when applying +15 A of charge current after discharging 18 Ah of capacity from a 60-Ah cell.

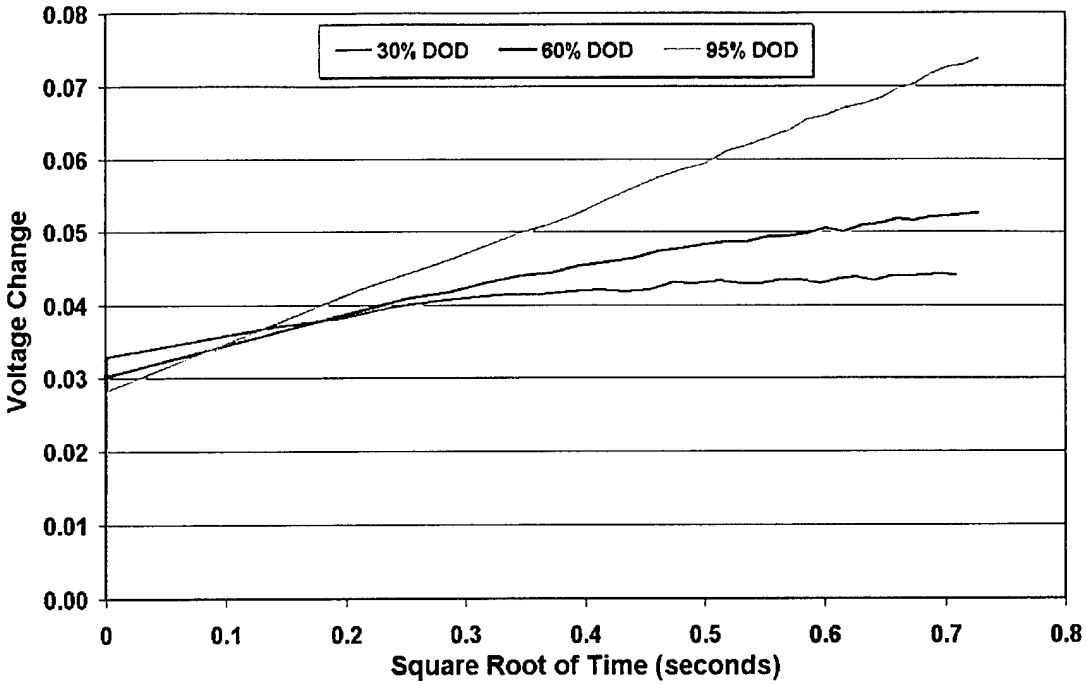


Figure 6. Voltage transients recorded at 10°C when applying +15 A of charge current after discharging 18 Ah of capacity from a 60-Ah cell.

Table 1. Resistances Obtained for a 60-Ah $NiH_2$ Cell at EOL for the Transition from C/4 Discharge to C/4 Charge

| SOC (%) | Temperature (°C) | $R_{cell}$ (mΩ | $R_{pol}$ (mΩ) |
|---|---|---|---|
| 100 | 10 | 1.034 | 0.282 |
| 55 | 10 | 1.034 | 0.415 |
| 10 | 10 | 0.987 | 0.712 |
| 5 | 10 | 0.988 | 1.077 |
| 100 | 0 | 1.033 | 0.610 |
| 55 | 0 | 1.033 | 0.850 |
| 5 | 0 | 1.008 | 1.603 |

As expected, the value of $R_{cell}$ does not vary significantly with state of charge or current because this is simply the resistance of the internal cell leads and the electrolyte between the electrodes in the cell. It also displays little variation with temperature for this cell because the positive temperature coefficient of the electrolyte is essentially offset by the negative temperature coefficient of the nickel leads. This may not be true for all cells and will depend on the relative contributions of leads and electrolyte to the ohmic cell resistance.

The value of $R_{pol}$ does vary significantly with both state of charge and temperature. It increases as the cell is discharged and as the cell temperature is decreased. A drop in temperature of 10°C appears to more than double the polarization resistance.

## 5. Battery Voltage Ripple Implications

Assuming that battery loads vary with approximately a 1-s period and have an amplitude of about C/2 when the battery passes from discharge to recharge (penumbral transit), the resistances reported in Table 1 can be used to estimate battery voltage ripple, $\Delta V$.

$$\Delta V = \Delta I \, (R_{batt} + N \, R_{pol}), \tag{1}$$

where N is the number of series-connected cells in the battery, and $R_{batt}$ corresponds to the high-frequency resistance of the battery (typically measured at 500 Hz). For a battery consisting of 22 cells, such as that tested here, and negligible additional wiring resistance, $R_{batt} = 22 \, R_{cell}$. For other types of batteries that do not use individual pressure vessel cells, such as single pressure vessel (SPV) batteries, the measured $R_{batt}$ may be used in Eq. 1.

Table 2 provides some estimates of the voltage ripple expected over the range of test conditions used here, assuming a 22-cell battery with no added wiring resistance. Additional wiring in the battery or higher ohmic battery resistance could increase the resistance and give more voltage ripple.

Table 2. Voltage Ripple Estimates for a 22-Cell 60-Ah $NiH_2$ Battery with No External Cell Wiring Resistance

| SOC (%) | Temperature (°C) | $R_{batt}$ (mΩ) | 22 x $R_{pol}$ (mΩ) | ΔV (V) |
|---|---|---|---|---|
| 100 | 10 | 22.75 | 6.20 | 0.868 |
| 55 | 10 | 22.75 | 9.13 | 0.956 |
| 10 | 10 | 21.71 | 15.66 | 1.121 |
| 5 | 10 | 21.74 | 23.69 | 1.363 |
| 100 | 0 | 22.73 | 13.42 | 1.084 |
| 55 | 0 | 22.73 | 18.70 | 1.243 |
| 5 | 0 | 22.18 | 35.27 | 1.723 |

## 4. Conclusions

The design of all satellite power systems should include sufficient voltage regulation to be tolerant of ripple caused by worst-case load fluctuations during penumbral transit.

The voltage ripple expected in a satellite power system should be estimated based on the measurement methods described here, and using the worst-case load fluctuations possible in the power system during penumbral transit. This estimate should be made at the lowest expected battery temperature and the highest DOD, and should be based on the performance of an end-of-life battery, such as that tested here. The system should then be designed to tolerate the worst-case voltage ripple that could result. For the operating conditions discussed here, such ripple can easily be over 1 V, but is not likely to exceed 1.5 V.

## LABORATORY OPERATIONS

The Aerospace Corporation functions as an "architect-engineer" for national security programs, specializing in advanced military space systems. The Corporation's Laboratory Operations supports the effective and timely development and operation of national security systems through scientific research and the application of advanced technology. Vital to the success of the Corporation is the technical staff's wide-ranging expertise and its ability to stay abreast of new technological developments and program support issues associated with rapidly evolving space systems. Contributing capabilities are provided by these individual organizations:

**Electronics and Photonics Laboratory:** Microelectronics, VLSI reliability, failure analysis, solid-state device physics, compound semiconductors, radiation effects, infrared and CCD detector devices, data storage and display technologies; lasers and electro-optics, solid-state laser design, micro-optics, optical communications, and fiber-optic sensors; atomic frequency standards, applied laser spectroscopy, laser chemistry, atmospheric propagation and beam control, LIDAR/LADAR remote sensing; solar cell and array testing and evaluation, battery electrochemistry, battery testing and evaluation.

**Space Materials Laboratory:** Evaluation and characterizations of new materials and processing techniques: metals, alloys, ceramics, polymers, thin films, and composites; development of advanced deposition processes; nondestructive evaluation, component failure analysis and reliability; structural mechanics, fracture mechanics, and stress corrosion; analysis and evaluation of materials at cryogenic and elevated temperatures; launch vehicle fluid mechanics, heat transfer and flight dynamics; aerothermodynamics; chemical and electric propulsion; environmental chemistry; combustion processes; space environment effects on materials, hardening and vulnerability assessment; contamination, thermal and structural control; lubrication and surface phenomena. Microelectromechanical systems (MEMS) for space applications; laser micromachining; laser-surface physical and chemical interactions; micropropulsion; micro- and nanosatellite mission analysis; intelligent microinstruments for monitoring space and launch system environments.

**Space Science Applications Laboratory:** Magnetospheric, auroral and cosmic-ray physics, wave-particle interactions, magnetospheric plasma waves; atmospheric and ionospheric physics, density and composition of the upper atmosphere, remote sensing using atmospheric radiation; solar physics, infrared astronomy, infrared signature analysis; infrared surveillance, imaging and remote sensing; multispectral and hyperspectral sensor development; data analysis and algorithm development; applications of multispectral and hyperspectral imagery to defense, civil space, commercial, and environmental missions; effects of solar activity, magnetic storms and nuclear explosions on the Earth's atmosphere, ionosphere and magnetosphere; effects of electromagnetic and particulate radiations on space systems; space instrumentation, design, fabrication and test; environmental chemistry, trace detection; atmospheric chemical reactions, atmospheric optics, light scattering, state-specific chemical reactions, and radiative signatures of missile plumes.